analytical chemistry

Article

pubs.acs.org/ac

Highly Efficient Enrichment Method for Glycopeptide Analyses: Using Specific and Nonspecific Nanoparticles Synergistically

Yali Wang,[†] Minbo Liu,[†] Liqi Xie,[‡] Caiyun Fang,[†] Huanming Xiong,*[,†] and Haojie Lu*[,†,‡]

[†]Department of Chemistry, Fudan University, Shanghai 200433, P. R. China

[‡]Key Laboratory of Glycoconjuates Research Ministry of Public Health and Institutes of Biomedical Sciences, Fudan University, Shanghai 200032, P. R. China

Supporting Information

ABSTRACT: We invented a new method for highly efficient and specific enrichment of glycopeptides using two different nanomaterials synergistically. One is boronic-acid-functionalized Fe_3O_4 nanoparticles, enriching glycopeptides through formation of cyclic boronate esters between the boronic acid groups and the cis−diol groups on glycopeptides. The other nanomaterial is conventional poly(methyl methacrylate) nanobeads, which have strong adsorption toward nonglycopeptides. By optimizing the proportion of these two materials, extremely high sensitivity and selectivity are achieved in analyzing the standard glycopeptides/nonglycopeptides mixture solutions. Since the washing step is not necessary for these conditions, the enrichment process is simplified and the recovery efficiency of target glycopeptides reaches 90%. Finally, this approach is successfully applied to analyze human serum with the sample volume as little as 1 μL, in which 147 different N-glycosylation peptides within 66 unique glycoproteins are identified. All these performances by the synergistic enrichment are much better than employing one specific enrichment agent alone.

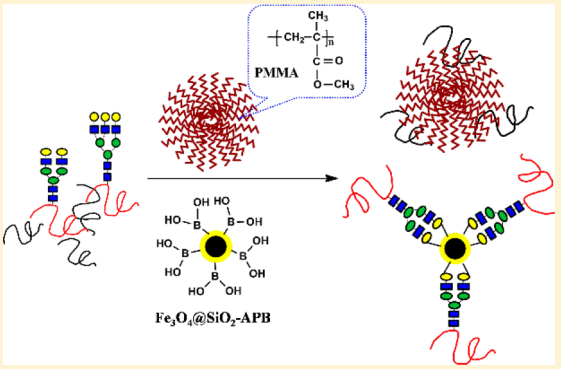

Glycosylation, as one of the most common and important post-translational modifications of proteins, is involved in many physiological functions and biological pathways, including protein folding, intracellular sorting, secretion, uptake, and cell recognition.[1−3] More than half of the discovered cancer biomarkers are glycosylated proteins or peptides, and it has been proven that the carbohydrate changes are closely related with the initiation and progression of tumors.[2] In glycoproteome research, mass spectrometry (MS) is a key technology in unraveling the biological functions of glycosylation.[4] However, the inherently low abundance of glycopeptides, the microheterogeneity of each glycosylation site, and the ion suppression effect caused by the coexistence of nonglycopeptides make the detection of glycopeptides extremely difficult in MS measurements.[5] Therefore, preconcentration and isolation of the target glycopeptides from the complex samples are indispensable before MS measurement.

Many methods have been developed for glycopeptide enrichment, such as lectin affinity,[6−8] size exclusion,[9,10] hydrazide chemistry,[11−13] and hydrophilic interaction chromatography.[14,15] Among them, the boronic-acid-based enrichment method has gained increasing attention,[16,17] because this method is unbiased to both N- and O-glycopeptides, facile to handle, and reversible for the glycopeptide alterations. Several types of material modified with boronic acid groups, including agarose resin,[18] mesoporous silica,[19,20] magnetic nanoparticles,[21] and monoliths,[22] have been reported for glycopeptide enrichment. However, employing these materials to enrich glycopeptides from practical samples has two main drawbacks. One is that sensitivity and selectivity are not satisfying because the boronic acid groups cannot cover the surface of these materials completely due to synthetic limitations, and thus, these materials also adsorb plenty of nonglycopeptides which are dominant in the practical sample solutions.[20,23] The other drawback, loss of target information, results from the typical enrichment operation which usually includes three steps: incubation, wash, and elution. In the washing step, several kinds of buffer solutions are optionally applied to wash off the nonspecific targets, causing inevitable loss of target molecules. In a practical biological sample digested by enzymes, the composition is extremely complicated and the concentrations of the target molecules are extremely low. Therefore, it is a great challenge to get sufficient valuable information of glycosylation from practical biological samples such as serum and tissues,[24] which relies on the development of highly sensitive and selective enriching methods.

In the present research, we invent a novel method to improve both sensitivity and selectivity of glycopeptide enrichment and avoid target loss in the meantime. This method employs two kinds of enriching materials. One is the

Received: October 8, 2013
Accepted: January 28, 2014
Published: January 28, 2014

   dx.doi.org/10.1021/ac403236q | *Anal. Chem.* 2014, 86, 2057−2064

Scheme 1. Schematic Illustration of the (a) Synthetic Procedure for the Fe_3O_4@SiO_2-APB Nanoparticles and the (b) Synergistic Enrichment Process for the Glycopeptides Using Fe_3O_4@SiO_2-APB Nanoparticles and PMMA Nanoparticles

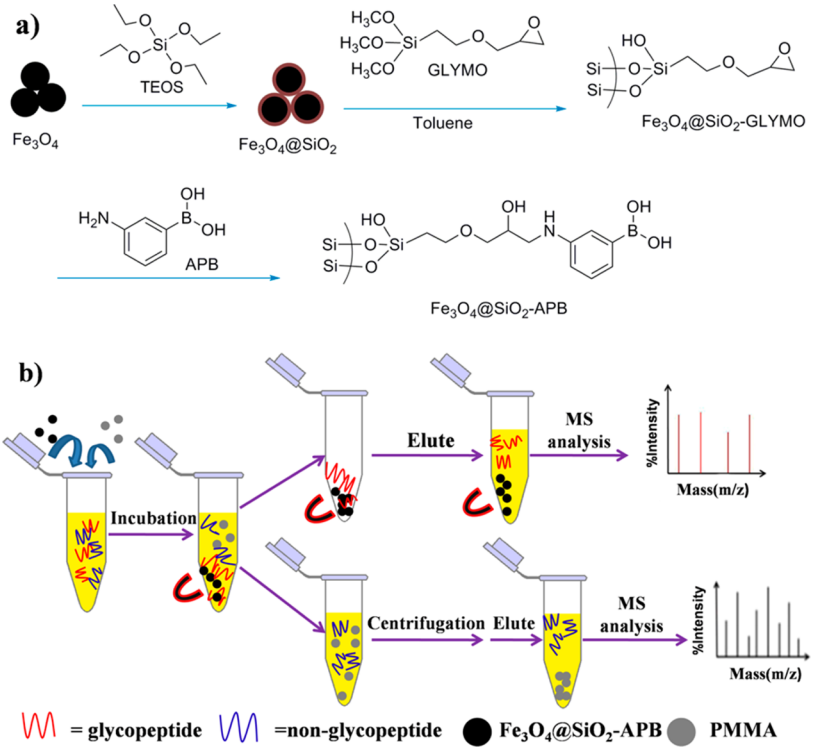

Fe_3O_4@SiO_2 core–shell nanoparticles modified with boronic acid groups (designated as Fe_3O_4@SiO_2-APB). The other is the conventional poly(methyl methacrylate) (PMMA) nanobeads, which have strong adsorption toward nonglycopeptide owing to their hydrophobic surfaces.[25,26] To the best of our knowledge, enriching glycopeptides by synergistic effect of different materials has not been reported yet. Although previous research reported that Fe_3O_4@SiO_2-APB was able to enrich glycopeptides efficiently,[21,27] the simultaneously adsorbed nonglycopeptides often disturbed the final MS analyses. Washing the nonglycopeptides off the Fe_3O_4@SiO_2-APB surface could improve the MS signal/noise ratio but also render the loss of target molecules. Especially when the concentration of target molecules was extremely low, some key information of the practical samples will be totally lost. However, when the PMMA nanobeads are added into the enrichment systems, situations are changed dramatically. PMMA is able to adsorb most of the nonglycopeptides and almost no glycopeptides after optimizing the ratio between Fe_3O_4@SiO_2-APB and PMMA. Furthermore, the washing step is never necessary. Therefore, the synergistic enrichment method has overcome the two drawbacks of the traditional enriching routes, and its application in human serum samples is very successful.

EXPERIMENTAL SECTION

Materials and Chemicals. Iron chloride hexahydrate ($FeCl_3$·$6H_2O$), 1,6-hexamethylenediamine, sodium acetate (NaAc), ethylene glycol (EG), anhydrous ethanol, aqueous ammonia solution (25 wt %), tetraorthosilicate (TEOS), 3-glycidyloxypropyltrimethoxysilane (GLYMO, 98%), 3-aminophenylboronic acid monohydrate (APB, 98%), methyl methacrylate (MMA), myoglobin (MYO, 95%), horseradish peroxidase (HRP, 98%), ammonium bicarbonate (ABC, 99.5%), dithiothreitol (DTT, 99%), iodoacetamide (IAA, 99%), acetonitrile (ACN, 99.9%), and trifluoro-acetic acid (TFA, 99.8%) were purchased from Sigma. Sequencing grade modified trypsin was from Promega. PNGaseF was obtained from New England Biolabs. All these reagents were used as received without further purification. SiMAG-boronic acid (magnetic silica particles functionalized with boronic acid) was purchased from Chemicell. Deionized water used for all experiments was obtained from a Milli-Q system (Millipore, Bedford, MA).

Synthesis of Fe_3O_4@SiO_2 Core–Shell Nanoparticles (NPs). The synthesis route of Fe_3O_4@SiO_2-APB NPs and PMMA NPs is illustrated in Scheme 1a. The magnetic Fe_3O_4 nanoparticles were synthesized through a hydrothermal reaction.[28] Briefly, 1.0 g of $FeCl_3$·$6H_2O$ was first dissolved in 30 mL of ethylene glycol under magnetic stirring. A clear yellow solution was obtained after stirring for 0.5 h. Then 3.60 g of 1,6-hexamethylenediamine and 4.0 g of sodium acetate were added to this solution which would turn brown. After being stirred for another 1 h, the resulting solution was transferred into a Teflon-lined stainless-steel autoclave. The autoclave was sealed and heated at 200 °C for 6 h and cooled to room temperature. The black magnetic nanoparticles were collected with the help of an external magnet field, followed by washing with ethanol, and deionized water several times.

The magnetic Fe_3O_4@SiO_2 core–shell nanoparticles were prepared according to the method by Deng et al.[29] The obtained Fe_3O_4@SiO_2 core–shell microspheres were redispersed in 50 mL of ethanol for further use.

Synthesis of Fe_3O_4@SiO_2-APB Nanoparticles. For synthesizing the boronic-acid-functionalized core–shell magnetic nanoparticles, we improved the two-step post graft method reported by Xu et al.[19] First, 50 mg of Fe_3O_4@SiO_2 core–shell nanoparticles were resuspended in 40 mL of

dx.doi.org/10.1021/ac403236q | Anal. Chem. 2014, 86, 2057–2064

methylbenzene containing 400 μL of GLYMO. Subsequently, the suspension was refluxed at 80 °C for 12 h. Finally, the nanocomposites were washed with ethanol three times to ensure the complete removal of excess GLYMO. Afterward, APB (50 mg) was dissolved completely in 60 mL of 50 mM NH_4HCO_3 (pH > 8) under ultrasonication. Then, 50 mg of Fe_3O_4@SiO_2-GLYMO were mixed with the above 20 mL of APB solution in a flask at 65 °C for 3 h with stirring, and then the supernatant were discarded with the aid of external magnet. After the supernatant was removed, 20 mL of APB solution was added into the flask to restart the reaction. This procedure as described above was repeated twice to prepare the final product Fe_3O_4@SiO_2-APB .

Synthesis of PMMA Nanoparticles. In a typical preparation of polymer beads, 10 g of MMA monomer and 150 mL of distilled water were mixed together and heated with stirring under nitrogen atmosphere for 30 min. When the temperature rose to 75 °C, 0.5 g of $K_2S_2O_8$ initiator was added to the reaction system. After reaction for 8 h, the mixture was cooled down to room temperature. The obtained milky suspension was PMMA nanobeads.[30]

Trypsin Digestion of Standard Proteins and Protein Mixture from Human Serum. The standard protein (HRP and MYO) solutions were dissolved, respectively, in 50 mM ABC buffer and denatured at 100 °C for 10 min. After cooling down to room temperature, Trypsin was added at an enzyme-to-substrate ratio of 1: 40 (w/w) and hydrolysis was proceeded overnight at 37 °C, respectively.

For the preparation of human serum digestion, 1 μL of human serum was diluted in lysis buffer (8 M urea, 60 mM ABC). The proteins were reduced with 10 mM DTT for 30 min at 60 °C and alkylated with 20 mM IAA at 37 °C for 30 min in the dark. The sample was then subjected to digestion, as described above. The obtained protein digestion was desalted on C18 columns and stored at −20 °C for further analysis.

Selective Enrichment of Glycopeptides by Fe_3O_4@SiO_2-APB and PMMA. The procedure of synergistic enrichment of glycopeptides is illustrated in Scheme 1b. Tryptic digests of HRP and MYO or peptides mixture from human serum were dissolved in 100 μL of loading buffer (50 mM ABC), then 10 μL of Fe_3O_4@SiO_2-APB suspension (10 μg/μL) and 20 μL of PMMA suspension (20 μg/μL) were added together and incubated at room temperature for 1 h. After that, the Fe_3O_4@SiO_2-APB nanobeads with captured glycopeptides were separated from the mixed solutions by applying an external magnet. Without any washing steps, the glycopeptides were released from Fe_3O_4@SiO_2-APB nanoparticles with 10 μL of elution buffer (20% ACN containing 1% TFA) directly for the subsequent MS analysis, while the PMMA nanobeads were collected by centrifugation at 14000 rpm for 3 min, and then treated directly by the above-mentioned elution buffer without washing for later MS measurement.

In our experiment, Fe_3O_4@SiO_2-APB and PMMA nanoparticles were added together into the complex sample of glycopeptides and nonglycopeptides. Hence, the ratio between Fe_3O_4@SiO_2-APB and PMMA was the key point. The optimization process of the ratio between these two materials was shown in Scheme 2. After incubation, Fe_3O_4@SiO_2-APB was separated by an external magnet, while PMMA was separated by centrifugation. Afterward, the peptides adsorbed on the nanoparticles were detected by the matrix-assisted laser desorption/ionization-time-of-flight-mass spectrometry (MALDI-TOF-MS). If the eluate from Fe_3O_4@SiO_2-APB

Scheme 2. Optimization Process for the Proportion between Fe_3O_4@SiO_2-APB (Designated as x) and PMMA Nanoparticles Applied in the Synergistic Enrichment

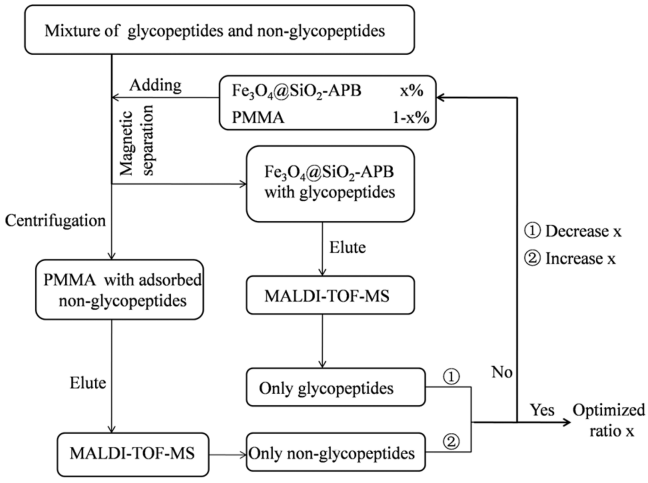

contained both glycopeptides and nonglycopeptides, we would decrease the proportion of Fe_3O_4@SiO_2-APB nanoparticles until no nonglycopeptides was detected in the final eluate. On the other hand, if the eluate from PMMA contained both nonglycopeptides and glycopeptides, we would decrease the proportion of PMMA until no glycopeptides were detected in the final eluate. Taking these two factors into account, the optimal ratio of these two materials was determined through constant adjustment until most glycopeptides were enriched by Fe_3O_4@SiO_2-APB and most nonglycopeptides were adsorbed by PMMA. After a series of parallel experiments, the optimal ratio of Fe_3O_4@SiO_2-APB and PMMA nanoparticles was found to be 1:4 (m/m) and adopted in the subsequent experiments.

MALDI Mass Spectrometric analysis. For the analysis of glycopeptides enriched from the tryptic digests mixture of HRP and MYO, 2 μL of eluate was dropped onto the MALDI plate, and then 1 μL of matrix solution (DHB at 12.5 mg/mL in a 0.1% (v/v) TFA and 50% (v/v) acetonitrile solution) was added for MS analysis. MALDI-TOF MS was performed by using an Axima MALDI-QIT-TOF MS instrument (Shimadzu Corp., Kyoto, Japan) with the nitrogen pulsed laser (337 nm). Spectra were obtained in positive ion mode using an accelerating voltage of 20 kV. MALDI MS data analysis was performed using Kompact.

Binding Capacity of the Synergistic Enrichment Method for Glycopeptides. To investigate the binding capacity, equivalent amounts of 100 μg Fe_3O_4@SiO_2-APB and 400 μg PMMA were incubated with 1 mL of tryptic HRP solution at different concentration for 1 h. Then, the supernatants which were separated from Fe_3O_4@SiO_2-APB by an external magnetic field were centrifuged at 14000 rpm for 1 min and the newly produced supernatants were analyzed by MALDI-TOF MS. The glycopeptides could only be detected when the total amount of HRP peptides was higher than the binding capacity of the synergistic enrichment method. Thus the binding capacity of the method could be estimated according to the minimum detected signals of glycopeptides.

Nano-Liquid Chromatography Tandem Mass Spectrometry (Nano-LC–MS/MS) Analysis of Glycopeptides. For the analysis of glycopeptides enriched from human serum protein mixture digestion, the eluate containing the enriched glycopeptides was lyophilized and then redissolved in 50 mM

dx.doi.org/10.1021/ac403236q | Anal. Chem. 2014, 86, 2057−2064

ABC buffer. For deglycosylation, 1 μL of PNGase F was added into the peptides solution, which was digested from 1 mg crude proteins, and the deglycosylation proceeded at 37 °C for 16 h. The deglycosylated peptides were then subjected to nano-LC–MS/MS analysis. Nano-LC–MS/MS was performed on an high-performance liquid chromatography (HPLC) system composed of two LC-20AD nanoflow LC pumps, an SIL-20 AC autosampler, and an LC-20AB microflow LC pump (Shimadzu,Tokyo, Japan) connected to an LTQ-Orbitrap mass spectrometer (ThermoFisher, San Jose, CA). The sample was loaded onto a CAPTRAP column (0.5 × 2 mm, MICHROM Bioresources, Auburn, CA) in 4 min at a flow rate of 25 μL min^{-1}. The sample was subsequently separated by a C18 reverse-phase column (0.10 × 150 mm, packed with 3 μm Magic C18-AQ particles, MICHROM Bioresources, Auburn, CA) at a flow rate of 500 nL min^{-1}. The mobile phases were 2% ACN with 0.1% FA (phase A) and 95% ACN with 0.1% FA (phase B). To achieve proper separation, a 90 min linear gradient from 0 to 45% phase B was employed. The separated sample was introduced into the mass spectrometer via an ADVANCE 30 μm silica tip (MICHROM Bioresources, Auburn, CA). The spray voltage was set at 1.8 kV, and the heated capillary was set at 180 °C. The mass spectrometer was operated in data-dependent mode and each cycle of duty consisted of one full-MS survey scan at a mass range of 385–2000 Da with a resolution power of 100000, using the Orbitrap section, followed by MS/MS experiments for the 10 strongest peaks using the LTQ section. The AGC expectation during full MS and MS/MS was 1 × 10^6 and 10000, respectively. Peptides were fragmented in the LTQ section using collision-induced dissociation with helium and the normalized collision energy value set at 35%. Previously fragmented peptides were excluded for 60 s.

Database Search. The data derived from the ESI-MS/MS analyses were searched by SEQUEST, against a composite database, including both original and reversed human protein database of international protein index (Combine. human. uniprot. sprot. 090210. fasta).[5] The parameters for the SEQUEST search were as follows: enzyme: trypsin; missed cleavages: one; fixed modification: carboxyamidomethylation (C); variable modifications: deamidation (N) and oxidation (M); peptide tolerance: 10 ppm; MS/MS tolerance: 1.0 Da. Furthermore, database search results were statistically analyzed using Trans-Proteomic Pipeline (TPP), which effectively computed the probability for the likelihood of each identification being correct in a data-dependent fashion. PeptideProphet would give high-confidence spectrum to peptide interpretation (score ≥ 0.90), and only those peptides that passed the peptide probability threshold of 0.95 can be accepted for further data interpretation. The Asn modification that did not occur in the N-X-S/T motif (X ≠ P) was eliminated to ensure the false positive rate below 1% for the identified glycosylation sites.

Characterization. The morphology and structure of Fe_3O_4@SiO_2-APB nanoparticles and PMMA nanobeads were examined by a JEM-2100F field-emission transmission electron microscopy (TEM) at an accelerating voltage of 200 kV and a Hitachi S-4800 Field-emission scanning electron microscopy (FE-SEM) at an accelerating voltage of 20 kV, respectively. FT-IR spectra were measured by a Nicolet Nexus 470 FT-IR spectrometer. Magnetic characterization was carried out with a vibrating sample magnetometer (VSM) on a model 6000 physical property measurement system (Quantum) at 300 K.

RESULTS AND DISCUSSION

Material Characterization. The size and morphology of the resulting Fe_3O_4@SiO_2-APB and PMMA nanoparticles were investigated by SEM and TEM, as shown in Figure 1. The

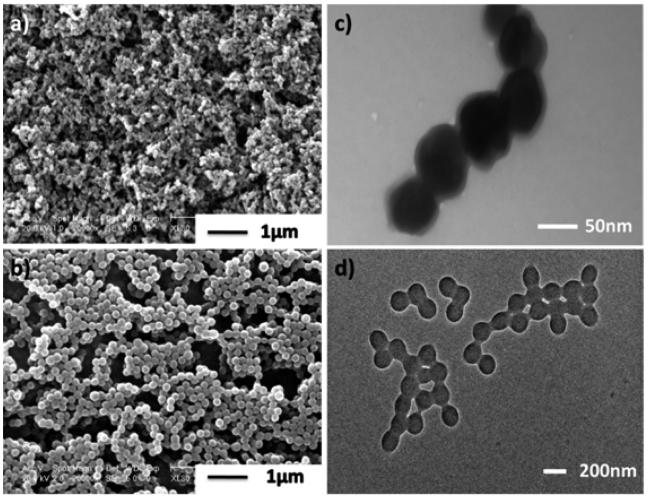

Figure 1. SEM images of (a) Fe_3O_4@SiO_2-APB nanoparticles and (b) PMMA nanoparticles. TEM images of (c) Fe_3O_4@SiO_2-APB nanoparticles and (d) PMMA nanoparticles.

obtained Fe_3O_4@SiO_2-APB core–shell nanoparticles were uniform and well-dispersed, with a mean diameter of about 70 nm (Figure 1, panels a and c). In addition, Figure 1c showed that each dark Fe_3O_4 core was coated tightly by a uniform gray silica shell with a thickness of about 10 nm. The SEM and TEM images of PMMA exhibited that such nanobeads had an average diameter of about 200 nm and they were spherical in shape and monodispersed in solvent (Figure 1, panels b and d). The PMMA suspension in water was very stable because of the electrostatic repulsion between the negatively charged PMMA nanobeads, which benefits their application in peptide adsorption.[25]

The surface modification of Fe_3O_4@SiO_2-APB nanoparticles were investigated by Fourier- transform-infrared (FT-IR) spectroscopy. In Figure 2a, the peak at 575 cm^{-1} was ascribed to the Fe–O vibrations, and a broad adsorption band at around

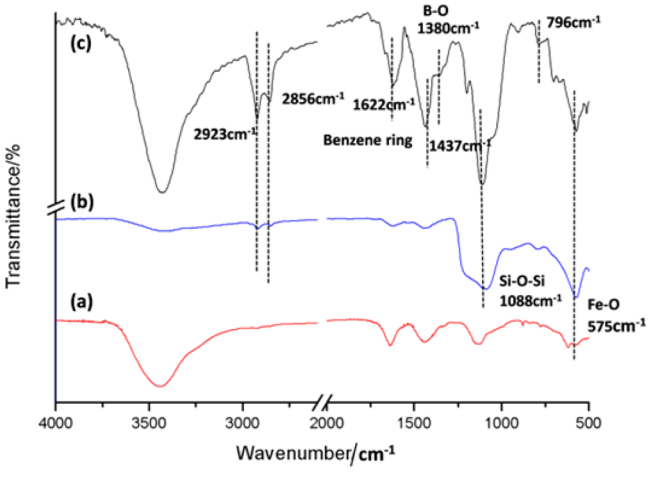

Figure 2. FT-IR spectra of (a) Fe_3O_4, (b) Fe_3O_4@SiO_2, and (c) Fe_3O_4@SiO_2-APB.

dx.doi.org/10.1021/ac403236q | Anal. Chem. 2014, 86, 2057–2064

3400 cm^{-1} was assigned to the O−H stretching vibrations. The band at 1088 cm^{-1} in Figure 2b, indication of the stretching vibration of Si−O−Si, confirmed the existence of silica shells around Fe_3O_4 cores. After modification with GLYMO, new IR peaks at 2856 and 2923 cm^{-1} were detected, which were assigned to the $-CH_2$ absorption from the silane agent GLYMO. In addition, IR bands at 1622, 1437, and 796 cm^{-1} were attributed to benzene ring stretching vibrations and *m*-benzene ring distorting vibrations, respectively. The successful functionalization of APB was evidenced by the presence of the B−O stretching mode at 1380 cm^{-1}, as shown in Figure 2c.

The magnetic properties of the as-prepared Fe_3O_4@SiO_2-APB nanoparticles were measured by a vibrating sample magnetometer (VSM) at room temperature. As shown in Figure S1 of the Supporting Information, the saturation magnetization (Ms) values of Fe_3O_4, Fe_3O_4@SiO_2, and Fe_3O_4@SiO_2-APB were 94.46, 52.71, 49.70 emu/g, respectively. The hysteresis curves indicated that all of the three species exhibited nearly superparamagnetic features. After coating SiO_2, the Ms value of Fe_3O_4 nanoparticles was sharply reduced but still remained with strong magnetic responsivity. The Ms value of the final Fe_3O_4@SiO_2-APB was a little lower than Fe_3O_4@SiO_2 due to the chemical modification on the surface. These results confirmed the formation of boronic-acid-functionalized core−shell nanoparticles.

The content of the B element was determinated by inductively coupled plasma-atomic emission spectrometry (ICP-AES). The concentration of B in the Fe_3O_4@SiO_2-APB was 1.5×10^{-4} mol/g, which was similar to that in the boronic-acid-functionalized MCM-41-APTES-CPB nanoparticles[20] but less than that in the SnO_2@Poly(HEMA-co-St-co-VPBA).[31] The SnO_2@Poly(HEMA-co-St-co-VPBA) nanoparticles were synthesized through a copolymerization route, which modified plenty of boronic acid groups on the nanoparticle surfaces, while in the present research, boronic acid groups were grafted onto Fe_3O_4@SiO_2 through a ring-opening reaction which was limited by the steric and diffusive barriers of the reactants.

Specific Enrichment of Glycopeptides. The traditional enrichment method includes three steps: incubation, washing, and elution. Organic or inorganic buffers are often employed to wash off the nonspecific molecules, but in the meantime, loss of some target molecules is inevitable. However in the present research, the washing step is discarded so that the loss of the glycopeptides is avoided and both time and labor are saved. At first, the standard tryptic digestion of HRP is used to evaluate the synergistic enrichment effects toward glycopeptides. There are theoretically 8 glycopeptides containing 9 glycosylation sites in HRP which dominate the mass spectrum; XylMan3FucGlcNAc2 accounts for more than 70% of the glycans.[32] Due to the specialty of the matrix-assisted laser desorption/ionization-quadrupole ion trap-mass spectrometry (MALDI-QIT-MS), the glycan chain would be broken at different positions and there might be more than 8 glycopeptide signals to be detected.[33] All of the glycopeptides detected in our experiments are listed in Table S1 of the Supporting Information.

The enrichment effects on the standard samples by different enriching agents are compared in Figure 3. Direct analysis of 0.1 ng/μL tryptic HRP digestion by MALDI-MS shows no signals in Figure 3a, but after enrichment by Fe_3O_4@SiO_2-APB, 3 peaks matching with the glycopeptides appear in Figure 3b. When a combination of Fe_3O_4@SiO_2-APB and PMMA is applied, the number of the peaks assigned to glycopeptides increases to 13 dramatically in Figure 3c. Peak 5 at m/z = 2591,

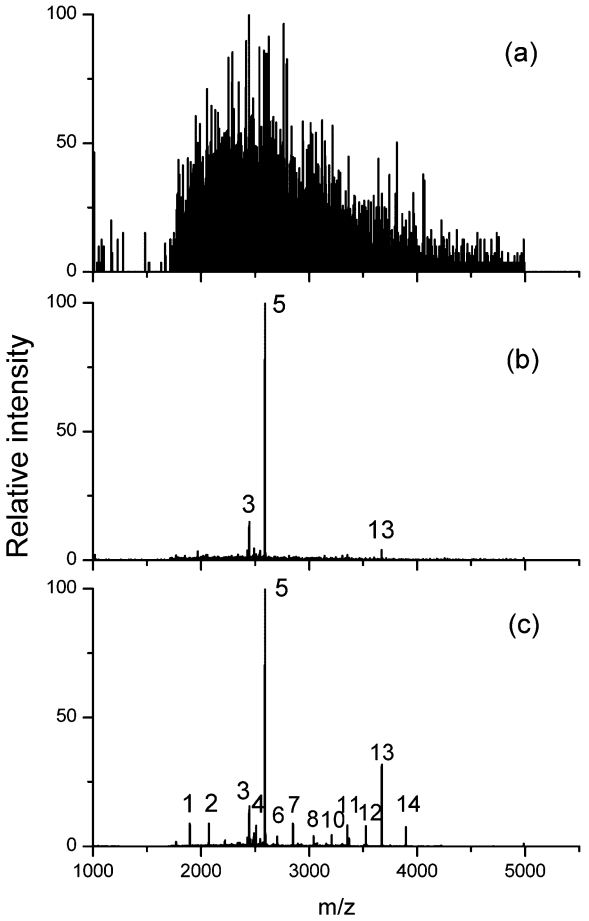

Figure 3. MALDI-QIT mass spectra of the tryptic digest of 0.1 ng/μL HRP: (a) without enrichment, (b) after enrichment by Fe_3O_4@SiO_2-APB nanoparticles, and (c) after synergistic enrichment (glycopeptide peaks are labeled with Arabic numbers).

which shows the strongest intensity in QIT mass spectrum, is a fragment generated from m/z = 4983, containing one complete N-glycan moiety at N_{216}. Peaks marked with 1, 4, and 9 (m/z = 1895, 2507, and 3074, respectively) are peptide fragments generated from peak 14 at m/z = 3895, corresponding to the peptide L_{69}-R_{92} with a N-glycan structure XylMan3FucGlcNAc2 at N_{87}. Peak 12 at m/z = 3525 is the fragment that loses fucose, which is generated from the peak 13 at m/z = 3671. In brief, the synergistic enrichment technique not only detects many more kinds of glycopeptides but also enhances their MS peak intensities greatly, which indicates that a higher sensitivity is realized.

After enlarging the mass spectrum in the range of m/z = 2600−5000, we can see that the overall MS intensity of the sample enriched by Fe_3O_4@SiO_2-APB alone is 0.3 mV (Figure S2b of the Supporting Information), while the overall MS intensity increases to 16 mV after employing the combination of Fe_3O_4@SiO_2-APB and PMMA (Figure S2c of the Supporting Information). Furthermore, the ratio of signal-to-noise (S/N) of Peak 13 (m/z = 3671) increase from 10 to 235. These results demonstrate clearly that the synergistic enrichment strategy is much more effective and sensitive than the traditional method using only one specific agent, Fe_3O_4@SiO_2-APB.

To evaluate the sensitivity of our strategy for glycopeptide enrichment, peak 6 at m/z = 2591 is chosen to determine the

dx.doi.org/10.1021/ac403236q | *Anal. Chem.* 2014, 86, 2057−2064

limit of detection (LOD). The S/N ratio is 55 in Figure 3c when the concentration of HRP digest is 2.23 fmol/μL (0.1 ng/μL), indicating that the detection limit of our method is at the subfmol level. To evaluate the selectivity of our strategy, the standard nonglycopeptides (tryptic digests of MYO) and the standard glycopeptides (tryptic digests of HRP) are mixed together with a molar ratio MYO/HRP = 100. Direct analysis on such mixture solution shows no glycopeptide signals (Figure 4a), while 6 glycopeptide peaks are detected after Fe_3O_4@SiO_2-APB enrichment (Figure 4b). When employing the combination of Fe_3O_4@SiO_2-APB and PMMA, 11 peaks related to glycopeptides are successfully detected with a very clean background in the mass spectrum (Figure 4c). This striking result is owing to the success of synergistic enrichment. In the traditional enrichment by Fe_3O_4@SiO_2-APB nanoparticles alone (Figure 4b), the washing step is required to remove the nonspecifically adsorbed peptides, which also renders loss of glycopeptides. In contrast, most of the nonglycopeptides are adsorbed by PMMA nanobeads in the synergistic enrichment and, thus, there is no need for washing off the nonglycopeptides from Fe_3O_4@SiO_2-APB (see Figure S2 of the Supporting Information). Moreover, Fe_3O_4@SiO_2-APB has more opportunities to capture glycopeptides due to the strong adsorption of PMMA nanobeads toward nonglycopeptides. As a result, the efficiency of glycopeptide enrichment is improved significantly.

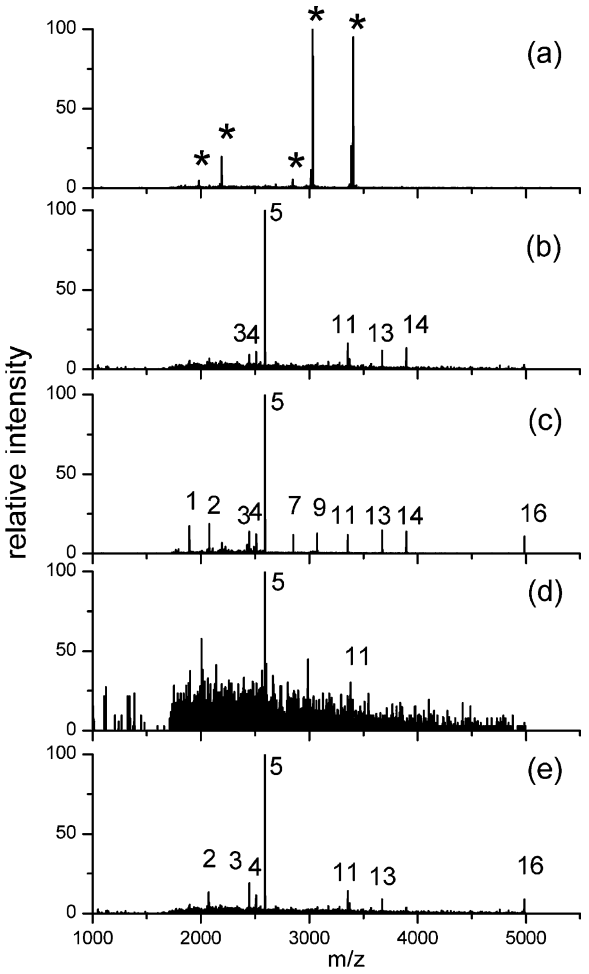

Figure 4. MALDI mass spectra of the tryptic digest mixture of HRP and MYO (with a molar ratio 1:100 of HRP to MYO): (a) without enrichment, (b) after enrichment by Fe_3O_4@SiO_2-APB, (c) after synergistic enrichment by Fe_3O_4@SiO_2-APB and PMMA, (d) after enrichment by commercial SiMAG-boronic acid, (e) after synergistic enrichment by commercial SiMAG-boronic acid and PMMA. (Glycopeptide peaks are labeled with Arabic numbers; nonglycopeptides are labeled with a "*").

For comparison, an equivalent amount of SiMAG-boronic acid (magnetic silica particles functionalized with boronic acid, purchased from Chemicell) is used to capture glycopeptides from the above-mentioned digested mixture. As shown in Figure 4d, there are only two glycopeptide signals with very weak intensity, while after a synergistic enrichment by SiMAG-boronic acid and PMMA nanobeads (Figure 4e), 7 peaks are detected and assigned to glycopeptides. Therefore, the synergistic enrichment not only shows better performances than the commercial enrichment materials but also exhibits universal improvement over the conventional methods.

In these years, boronic acid-functionalized materials have been discussed frequently in the field of glycopeptides or glycoproteins. Some advanced architecture, such as core–satellite composite[19] and denotation nanodiamond,[34] have been developed; however, the maximum selectivity of 1:40 for glycopeptides/nonglycopeptides is not satisfactory. Some researchers employed the copolymerization route to introduce the relatively large amount of the functional groups onto the surface of materials, such as SnO_2@poly (HEMA-co-St-co-VPBA)[31] and poly(MBA-co-MAA)@VPBA,[23] but they were mainly used in the standard samples or the high-abundant proteins in real biological sample. Recently, Liu et al.[20] reported a boronic acid-functionalized mesoporous silica MCM-41-APTES-CPB with excellent selectivity at a molar ratio of glycopeptides/nonglycopeptides of 1:100, but only 3 glycopeptides could be analyzed (for comparison, 11 glycopeptides detected in this presented synergistic method). By far, the synergistic method presents the highest selectivity for glycopeptides in the literature.

The binding capacity of the synergistic enrichment method was also studied. From Figure S4 of the Supporting Information, we can see that the binding capacity of the new method was calculated to be 150 mg/g. Compared with some other boronic-acid-functionalized materials such as MCM-41-APTES-CPB[20] and the core–satellite composite nanoparticles,[21] of which the binding capacities were 40 and 79 mg/g respectively, the synergistic enrichment method outperformed them greatly.

The recovery of glycopeptides from our approach was also investigated. A certain amount of tryptic digested HRP was divided equally into two parts. One was treated with trypsin in $H_2{}^{18}O$, which produced a 4 Da mass increase by introducing two ^{18}O atoms at the C-termini of the peptides. The other was treated with trypsin in $H_2{}^{16}O$. The ^{18}O labeled part was enriched by Fe_3O_4@SiO_2-APB and PMMA nanoparticles, while the ^{16}O-labeled part was not enriched. By mixing these two parts, we could compare the products by MS to study the abundances of the glycopeptides from different oxygen isotopes, according to the relative intensities of MS peaks.[35,36] The MALDI-TOF data revealed that the recovery of glycopeptides in synergistic enrichment was up to 90% (see Figure S5 of the Supporting Information), while the recovery of glycopeptides enriched by Fe_3O_4@SiO_2-APB alone was only 78%. This result further confirmed that adding PMMA saved the target glycopeptides tremendously and improved the enrichment performance of the boronic-acid-modified nano-

dx.doi.org/10.1021/ac403236q | Anal. Chem. 2014, 86, 2057–2064

particles. To our knowledge, it is the highest recovery among all of the boronic-acid based methods at present.

In order to test the new method practically, 1 μL of human serum as a complex sample was examined for identifying the glycopeptides and glycoproteins. The proteins extracted from human serum were digested with trypsin and incubated with the combination of Fe_3O_4@SiO_2-APB and PMMA for enriching glycopeptides. The eluted glycopeptides were then deglycosylated by PNGase F, and the deglycosylated peptides were subjected to nano-LC-MS/MS analyses. The identity of the N-glycosylated peptide was confirmed by the presence of a consensus N-X-S/T sequence, in which X could be any amino acid except Proline[37] and by deamidation on the asparagine residues using PNGase F (mass increment of 0.9858 Da). In a single LC−MS/MS run, 95 nonredundant glycopeptides with corresponding 101 glycosites [with N-X-S/T (X≠P) sequences] were identified, which corresponded to 44 glycoproteins (see Table S2 of the Supporting Information) after the traditional enrichment method by Fe_3O_4@SiO_2-APB alone. In contrast, a total of 147 glycopeptides with corresponding 153 glycosites [with N-X-S/T (X≠P) sequences] mapped to 66 different glycoproteins (listed in Table S3 of the Supporting Information) were identified via synergistic enrichment by the combination of Fe_3O_4@SiO_2-APB and PMMA. The number and ratio on the identification of nonglycosylated peptides in the serum was listed in Table S4 of the Supporting Information. All these results confirmed that the synergistic enrichment strategy is able to achieve better performance than using one specific enrichment material alone, especially for the identification of glycoproteins in real biological samples.

CONCLUSIONS

In summary, we proposed a novel synergistic enrichment of glycopeptides by utilizing two different nanoparticles: one is magnetic boronic-acid-functionalized core−shell nanoparticles (Fe_3O_4@SiO_2-APB) for capturing glycopeptides selectively and the other is polymer nanobeads (PMMA) for nonspecific adsorption of peptides. This innovative method has shown advantages in five aspects at least. First, it exhibits excellent sensitivity in detecting standard glycopeptides at a level of subfemtomol/microliter and greatly improves the S/N ratios in MALDI MS analyses. Second, it possesses good selectivity, even in a standard mixture solution with a molar ratio of nonglycopeptides/glycopeptides = 100. Third, it improves the recovery of glycopeptides up to 90%, which is the highest in the literature by far. Fourth, it can be applied to analyze only 1 μL of human serum and presents convincing results. Finally, it saves a lot of time and labor in treating samples before MS measurements. Most importantly, this synergistic enrichment approach has shown much better performances than using only one specific enrichment agent in all of the above-mentioned aspects. Therefore, the present study has set up a new enrichment method for analyzing glycopeptides with remarkable efficiency. We believe this method can be extended to other enrichment systems besides glycopeptides, in which one specific agent is employed to capture target molecules and the other nonspecific agent is employed to adsorb disturbing molecules synergistically.

ASSOCIATED CONTENT

Supporting Information

Additional information as noted in text. This material is available free of charge via the Internet at http://pubs.acs.org.

AUTHOR INFORMATION

Corresponding Authors

*E-mail: hmxiong@fudan.edu.cn. Tel: (086) 021-54237618. Fax: (086) 021-54237961.

*E-mail: luhaojie@fudan.edu.cn.

Notes

The authors declare no competing financial interest.

ACKNOWLEDGMENTS

The work was supported by the National Science and Technology Key Project of China (Grants 2012CB910602, 2012AA020203, 2012YQ12004409, and 2013CB934101), the National Science Foundation of China (Grants 21025519, 21335002, 21271045, and 21105015), the Ph.D. programs foundation of the ministry of education of China (Grant 20130071110034), and Shanghai Projects (Eastern Scholar and B109).

REFERENCES

(1) Nilsson, J.; Halim, A.; Grahn, A.; Larson, G. *Nat. Methods* **2009**, *6*, 809−811.

(2) Ohtsubo, K.; Marth, J. D. *Cell* **2006**, *126*, 855−867.

(3) Grewal, P. K.; Uchiyama, S.; Ditto, D.; Varki, N.; Le, D. T.; Nizet, V.; Marth, J. D. *Nat. Med.* **2008**, *14*, 648−655.

(4) Pan, S.; Chen, R.; Aebersold, R.; Brennall, T. A. *Mol. Cell. Proteomics* **2011**, *10*, 1−14.

(5) Ma, W.; Li, L.; Zhang, Y.; An, Q.; You, L.; Li, J.; Zhang, Y.; Xu, S.; Yu, M.; Guo, J.; Lu, H.; Wang, C. *J. Mater. Chem.* **2012**, *22*, 23981−23988.

(6) Kaji, H.; Saito, H.; Yamauchi, Y.; Shinkawa, T.; Taoka, M.; Hirabayashi, J.; Kasai, K.; Takahashi, N.; Isobe, T. *Nat. Biotechnol.* **2003**, *21*, 667−672.

(7) Wang, Y.; Wu, S.; Hancock, W. *Glycobiology* **2006**, *16*, 514−523.

(8) Qiu, R.; Regnier, F. *Anal. Chem.* **2005**, *77*, 2802−2809.

(9) Alvarez-Manilla, G.; Atwood; Guo, Y.; Warren, N.; Orlando, R.; Pierce, M. *J. Proteome Res.* **2006**, *5*, 701−708.

(10) Zielinska, D.; Gnad, F.; Mann, M. *Cell* **2010**, *141*, 897−907.

(11) Zhang, H.; Li, X.; Martin, D. B.; Aebersold, R. *Nat. Biotechnol.* **2003**, *21*, 660−666.

(12) Li, Y.; Tian, Y.; Rezai, T.; Prakash, A.; Lopez, M. F.; Chan, D.; Zhang, H. *Anal. Chem.* **2011**, *83*, 240−245.

(13) Zhang, Y.; Kuang, M.; Zhang, L.; Yang, P.; Lu, H. *Anal. Chem.* **2013**, *85*, 5535−5541.

(14) Selman, M.; Hemayatkar, M.; Deelder, A.; Wuhrer, M. *Anal. Chem.* **2011**, *83*, 2492−2499.

(15) Yu, L.; Li, X.; Guo, Z.; Zhang, X.; Liang, X. *Chem.—Eur. J.* **2009**, *15*, 12618−12626.

(16) Sparbier, K.; Koch, S.; Kessler, I.; Wenzel, T.; Kostrzewa, M. *Journal of Biomolecular Techniques* **2005**, *16*, 407−413.

(17) Liu, Y.; Ren, L.; Liu, Z. *Chem. Commun.* **2011**, *47*, 5067−5069.

(18) Zhang, Q.; Schepmoes, A.; Brock, J.; Wu, S.; Moore, R.; Purvine, S.; Baynes, J.; Smith, R.; Metz, T. *Anal. Chem.* **2008**, *80*, 9822−9829.

(19) Xu, Y.; Wu, Z.; Zhang, L.; Lu, H.; Yang, P.; Webley, P.; Zhao, D. *Anal. Chem.* **2009**, *81*, 503−508.

(20) Liu, L.; Zhang, Y.; Zhang, L.; Yan, G.; Yao, J.; Yang, P.; Lu, H. *Anal. Chim. Acta* **2012**, *753*, 64−72.

(21) Zhang, L.; Xu, Y.; Yao, H.; Xie, L.; Yao, J.; Lu, H.; Yang, P. *Chem.—Eur. J.* **2009**, *15*, 10158−10166.

(22) Sun, X.; Liu, R.; He, X.; Chen, L.; Zhang, Y. *Talanta* **2010**, *81*, 856−864.

(23) Qu, Y.; Liu, J.; Yang, K.; Liang, Z.; Zhang, L.; Zhang, Y. *Chem.—Eur. J.* **2012**, *18*, 9056−9062.

(24) Li, X.; Gong, Y.; Wang, Y.; Cai, Y.; He, P.; Lu, Z.; He, F.; Zhao, X.; Qian, X. *Mol. Cell. Proteomics* **2004**, *3*, 221−221.

(25) Chen, H.; Deng, C.; Zhang, X. *Angew. Chem., Int. Ed.* **2010**, *49*, 607−611.
(26) Xiong, H.; Guan, X.; Jin, L.; Shen, W.; Lu, H.; Xia, Y. *Angew. Chem., Int. Ed.* **2008**, *47*, 4204−4207.
(27) Zhang, X.; He, X.; Chen, L.; Zhang, Y. *J. Mater. Chem.* **2012**, *22*, 16520−16526.
(28) Deng, H.; Li, X.; Peng, Q.; Wang, X.; Chen, J.; Li, Y. *Angew. Chem., Int. Ed.* **2005**, *44*, 2782−2785.
(29) Deng, Y.; Qi, D.; Deng, C.; Zhang, X.; Zhao, D. *J. Am. Chem. Soc.* **2008**, *130*, 28−29.
(30) Xiong, H.; Xie, D.; Guan, X.; Tan, Y.; Xia, Y. *J. Mater. Chem* **2007**, *17*, 2490−2496.
(31) Shen, W.; Ma, C.; Wang, S.; Xiong, H.; Lu, H.; Yang, P. *Chem.−Asian J.* **2010**, *5*, 1185−1191.
(32) Wuhrer, M.; Hokke, C.; Deelder, A. *Rapid Commun. Mass Spectrom.* **2004**, 1741−1748.
(33) Qi, D.; Zhang, H.; Tang, J.; Deng, C.; Zhang, X. *J. Phys. Chem. C* **2010**, *114*, 9221−9226.
(34) Xu, G.; Zhang, W.; Wei, L.; Lu, H.; Yang, P. *Analyst* **2013**, *138*, 1876−1885.
(35) Yao, X.; Freas, A.; Ramirez, J.; Demirev, P. A.; Fenselau, C. *Anal. Chem.* **2001**, *73*, 2836−2842.
(36) Zang, L.; Toy, D.; Hancock, W.; Sgroi, D.; Karger, B. *J. Proteome Res.* **2004**, *3*, 604−612.
(37) Liu, X.; Ma, L.; Li, J. *Anal. Lett.* **2008**, *41*, 268−277.